THE NEUTRAL ATOMS DETECTOR TECHNOLOGIES DEVELOPED FOR THE SERENA PACKAGE IN VIEW OF ESA BEPICOLOMBO PLANETARY ORBITER.

A. M. Di Lellis [(1)], S. Orsini [(2)], S.Livi [(3)], P. Wurz [(4)], A. Milillo [(2)].
[(1)] AMDL S.r.l. - ROME, Italy, [(2)] IFSI/CNR, ROME ITALY, [(3)] JHUAPL LAUREL MD USA,
[(4)] PHYSIKALISHES INSTITUT UNIVERSITY OF BERN SWITZERLAND

A comprehensive suite for the particle detection in the Mercury environment, the SERENA instrument, is going to be proposed for the ESA cornerstone BepiColombo mission. The SERENA package consists of the sensors STROFIO and ELENA, which identify the neutral particles and measure their energies in the range from fractions of eV to a few keVs, and the sensors PICAM and MIPA for measuring and analyzing ionized particles from some eV to tens of keV.

The proposed neutral sensor STROFIO will observe and analyze the bulk of the thermal / supra-thermal (0-50 eV) exospheric gas along the ram direction, while ELENA will be devoted to detect the sputtering emission (E min < 100eV; E max > 1 keV) within 1-D (2 deg x 60 deg) nadir cross track slices from the planet surface. The paper describes the new design techniques approached for the neutral particles identification and the related miniaturized data-handling unit. Such design technologies could be fruitfully exported to different applications for planetary exploration.

THE NEUTRAL PARTICLE ANALYZERS SUITE

The Neutral and Ionized Particle Analyzer (NIPA-SERENA - Search for Exospheric Refilling and Emitted Natural Abundances-, hereafter called SERENA for simplicity) to be proposed on board the MPO consists of three spectrometers. Namely:

a) ELENA that investigates the Hermean escaping neutral gas (strongly linked to its surface), its dynamics and the processes responsible of such a population;
b) STROFIO that investigates the exospheric gas composition;
c) MIPA and/or PICAM ion spectrometer that investigate the chain of processes by which plasma precipitate toward the surface and ions are ejected from the soil together with the neutrals, which on their hand maybe photo-ionized and transported throughout the environment of Mercury.

The energy spectrum of neutral particles ranges from fractions of eV up to tens of keV. Such a large energy interval cannot be covered by a single detector; see for example the recent review by *Wurz,* (2000). The instrument is therefore based on a modular approach:

- the STROFIO detector measures the neutral particle composition at the lowest energy range (~0 to a few eV), and the particle density in the exosphere, with associated high voltage power supplies and front end electronics;
- the ELENA detector, covers the low (<20 eV – 5 keV) energy spectrum, with associated high voltage power supplies and front end electronics;
- a common electronics unit includes the data processing and buffering electronics, the low power converter and the command and data I/F to the MPO systems and to the ion spectrometers MIPA and/or PICAM .

The STROFIO detector measures the neutral particles with low energies (exospheric particles) and has no imaging capability. The analysis of the exospheric released gases allows indirect reconstruction of the surface composition, by processing successive measurements over several orbits.
The ELENA has a high resolution and 1-D field-of-view (perpendicular to the S/C orbital plane). This configuration allows a posteriori collection of the ELENA signal along each single orbit for reconstructing the global image of the plasma surrounding Mercury and its interaction with the surface.

1.1. STROFIO DESCRIPTION

STROFIO is a high mass resolution, time-of-flight system for low energy neutral particles. It can measure the chemical composition of low-pressure gases, the relative abundance of different species, and the particle flow direction and velocity. The design of the STROFIO sensor is driven by the attempt to achieve both isotopic resolving capability – of about $m/\ m = 60$ – and temporal resolution – a full spectrum can be acquired in 100ms – within very limited resources (1 kg, 1W). All atom species, as well as elements or isotopes can be detected within the mass resolution, including noble gases. Neutral particles are discriminated from ions by means of a collimator located at the sensor entrance. The FOV is 5° along the zenith-nadir direction, and 10° along the direction parallel to the local horizon. STROFIO performs integral measurements both in angular direction and energy (from ~0 to 10 eV). The mass spectral resolution is sufficient to resolve all expected elements as well as their isotopes. A nominal 100 s integration period will roughly correspond to a 5° variation of the anomaly at the pericenter. Taking into account the blurring of the low-energy particle trajectories, an actual pixel angular size of 10° will be obtained.

Proc. 37th ESLAB Symposium 'Tools and Technologies for Future Planetary Exploration', Noordwijk, The Netherlands, 2-4 December 2003 (ESA SP-543, February 2004)

1.1.1 Principle of Operation

The main components of the STROFIO sensor (shown in Figure 1) in order as they are traversed by an incoming ion are:

- Ionization source
- Focusing optic
- RF dispersing region
- Field free region
- 2D detector

As schematically shown in Figure 1, the neutral particles enter into the system through the first element, which ionizes the neutral gas. The ions are released into the focusing optic that then delivers a beam of ions to the RF dispersing system. Once the particles leave the dispersing region they move on a constant trajectory to the 2D MCP detector system where the time of flight is measured, from which the mass/charge can be calculated.

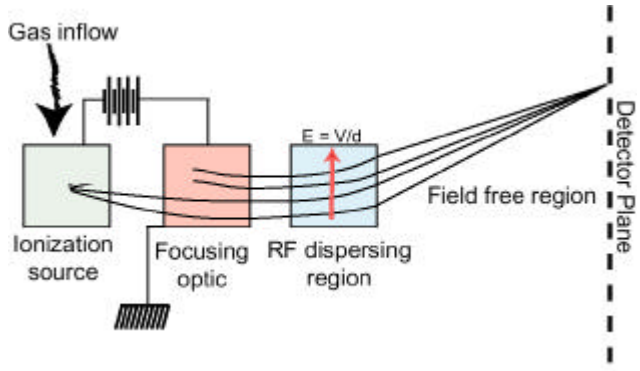

Figure 1. Schematic diagram of STROFIO

1.1.2 Ionizing Source and Focusing Optic

The design of the ion source is based on the electron bombardment sources used in modern laboratory rare gas mass spectrometers, for instance derived from the ionization source built for the Rosina experiment on the ESA Rosetta spacecraft (Balsiger et al, 1997). Neutral gas enters the ionization region perpendicular to the drawing plane. Ions are produced by electron bombardment and are extracted by a potential applied. The subsequent electrodes focus and accelerate the beam to its final energy. Suitable potentials applied to these electrodes prevent the entry of low energy ions into STROFIO, while ions of higher energy cannot reach the dispersing element.

1.1.3 RF Dispersing Element

The capability of STROFIO to separate different mass/charge ions relies on the effect of a rotating field on the trajectory of particles. Figure 2 illustrates the main principle: an ion enters the region from the left, where an electric field of magnitude V/d is present, perpendicular to the particle's velocity. The ion trajectory then follows a curve, contained in the plane defined by the incoming velocity and the direction of the electric field.

Consider now the effects of an electric field, constant in magnitude, but with direction rotating uniformly in space, in a plane perpendicular to the initial ion velocity, at a frequency f. Such a field can be generated by four electrodes, placed at a distance 2d from each other in a geometrical configuration as depicted in. At the electrode n (n=1…4) a potential V is applied is applied

The resulting electric field is constant in magnitude and equal to V/d. As the imposed electric field direction is varied in time, the trajectory within the dispersing electrodes will still be bounded to a plane, when the transit time through the electrodes is small compared to the period of the wave. Slower particles will experience an "effective field" that is the average of the electric field during the time taken to traverse the electrodes: the resulting change in perpendicular velocity will be smaller (average over time of the sinusoidal waveform), but the mass resolution capability will be retained (Clemmons and Herrero, 1998).

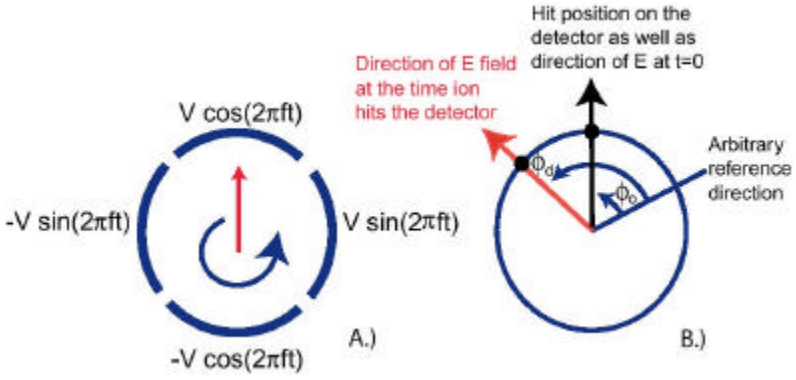

Figure 2. Functionality of the time rotating field.

The way this rotating field generates mass dispersion is readily explained in the case that the detector is a simple point detector, placed at the appropriate off-axis distance. The trajectory of an ion can hit the detector only if the field points to the detector while the ion traverses the dispersing region. At other times, the ion will simply miss the detector. The time difference between the instant when the particle arrives at the detector and the time when the field was pointing in the appropriate direction is equal to the travel time through the field free region. Since the ions have all about the same energy/charge (the acceleration voltage), this time-of-flight is directly proportional to the square root of the mass per charge. This possibility enables STROFIO to act as a correlated set of TOF spectrographs, recapturing the duty cycle losses associated with "point" detection.

The angular difference between the phase of RF electric field and the position on the ring uniquely determines the mass/charge of every ion.

1.1.4 Dimensional Detector

Two characteristics are important in defining the detection system: good timing and angular resolution. Results from the beam test (see Figure 3 have shown that for the chosen configuration, the overall peak spread is 48 ns. Microchannel plates exhibit a timing performance, typically of 1–2 ns, and are therefore the more suitable choice. A two dimensional

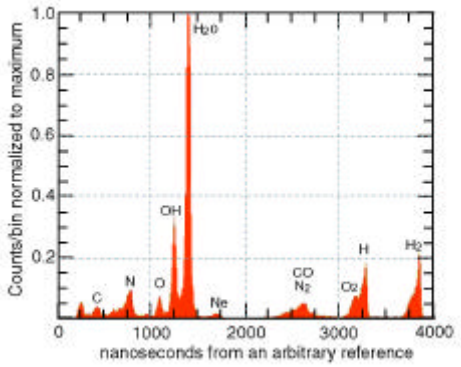

Figure 3. Beam Test . Dispersing electric field 3 V/mm. Length of the dispersion electrode 25 mm Length of the free-field region 193 mm. Lateral displacement of the beam 59mm. Frequency of the RF field 167,300 Hz Voltage on the first Einzel lens 72V Voltage on the second Einzel lens 43V Pressure in the vacuum chamber 2×10^{-6} Torr.

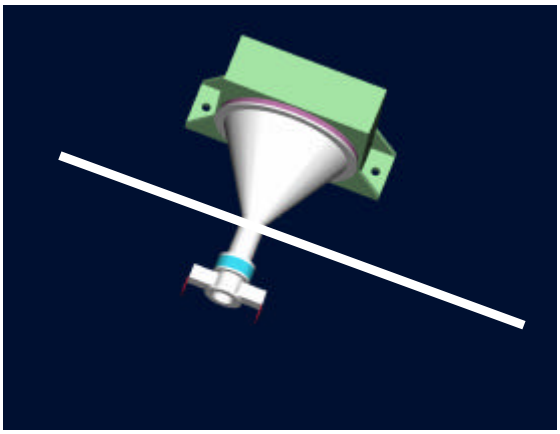

Figure 4. Layout of the STROFIO instrument front end. The two small bars at the bottom represent the entrance apertures. Only the vertical pipe has to be outside the s/c interface, which is indicated by a white line.

read-out can be achieved by discrete anode: here the major advantage lies in the complete independence of the different channels, which can be treated as single point detectors. The related front-end processing ASIC has been already identified, and it is able to support 128 channels in parallel, in spite of very low power consumption (< 70 mW). Alternatively a resistive anode and Wedge-Strip-and-Zig-zag detector could be used, i.e.: determination of the angular position is achieved by comparing analogue signals at the ends of the properly shaped resistive anode. The electronic is smaller (albeit more complex) and position accuracy can be high (of the order of 1º). The number of processed counts per second is quite limited, of the order of 100 kHz. The timing characteristics depend on the speed of the electronics.
The dimensions of STOFIO are about 15×15×30 cm (see Figure 4). The unit should be mounted on the S/C lateral side. The signal will enter the unit through two opposite apertures, respectively pointing toward the ram and the anti-ram directions. In this way, one of the two instrument entrances can always face the ram direction, independently from the specific S/C configuration. Only these entrance apertures have to be outside the body of the s/c and do not need special cooling. The apertures of the FOV (5°×10°) must however be unobstructed.

1.2. ELENA DESCRIPTION

The sensor ELENA (Emitted Low-Energy Neutral Atoms) is a Time-of-Flight Detector, based on the state-of-the art of ultra-sonic oscillating choppers (>100 kHz) and mechanical gratings.
The new development in this field allows unprecedented performances in timing discrimination against noise of low-flux neutral particles. The sensor concept is based on micro-valve choppers, which release the incoming neutral particles impinging on the detector entrance with a definite timing. Particles are then flown in a TOF chamber, and finally detected by a 2-dimesional array (based on MCPs and discrete anodes sets), allowing to reconstruct both energy and direction of the incoming events.
Even if multi-valves systems based on large-scaling integration piezoelectric bi-morphs MEMS are under investigation, in order to assess the maturity level actually requested for BepiColombo we have identified a more realistic ultra-sonic motor, already available in the hi-rel market. The chopping is achieved by coupling such a hi-frequency mechanical oscillator with hi-resolution grating technologies (see Figure 5).
The equivalent timing profile, for which shutters are subsequently opened and closed, is controlled by facing fixed and moving mechanical micro-windows. These are implemented by distributed sequences of pseudo-random openings. Then, according to the motor oscillations, particles are allowed to enter the TOF chamber, according to a definite pseudo-random temporal sequence. Hadamard transform of the signal sampled on the stop detector (Figure 8) allows full reconstruction of particles TOF (i.e.: velocity). The measured

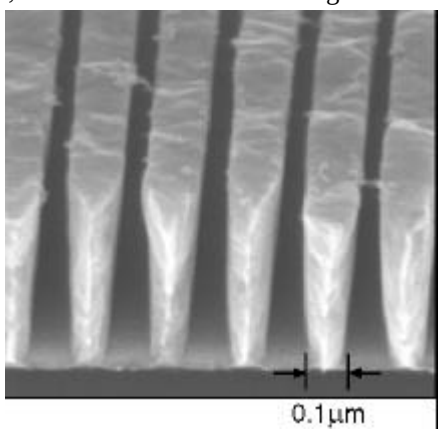

Figure 5. High resolution chopping grating (Courtesy of SNL/MIT)

velocity, together with a pulse-height analysis of the stop events energy, then allows also a zero order identification of the impinging particle mass.The motor is driven by a piezo-electric module at a frequency of about 100 kHz. The total moving assembly has a mass of <5 g.ELENA has a pixel intrinsic field-of-view (IFOV) of 32 mrad×32 mrad (~1.8°×1.8°). A one-dimensional FOV of 1024 mrad (~ 60°) is achieved with 32 pixels. The alignment of the 1-D view to the cross track direction provides:

- swath width (cross track, central 8 pixels): >102.96 km at 400 km altitude, 386.40 km at 1500 km
- swath length (along track, 1 pixel): > 12.87 km at 400 km, > 48.30 km at 1500 km.

For the baseline 400 km ×1500 km orbit, the pixel dwell time is about 4.95 s (pixel footprint: 12.87 km, ground velocity: ~2.6 km/s). The ELENA data points integrated over such a time should correspond to 32 angular pixels ×16 energies ×8 mass bins.

Mass bins should be chosen in order to discriminate light, medium and heavy species. On-board computation flexibility must be foreseen to bin and to integrate individual events and measure rates between 10^4 and 10^8 particles/(cm^2 s sr keV). An efficient UV rejection capability is achieved by properly sizing the above-mentioned gratings, to minimize performances degradation for an illumination up to 10^9 photons/(cm^2 s sr). Thanks to the very efficient duty cycle, achieved by pseudo-random shuttering (50%), an overall geometrical factor of at least 10^{-3} cm^2 sr keV can be obtained, with a 1 cm^2 entrance opening which will ensure that 50 to 5 x 10^5 events are accumulated during the given dwell time.

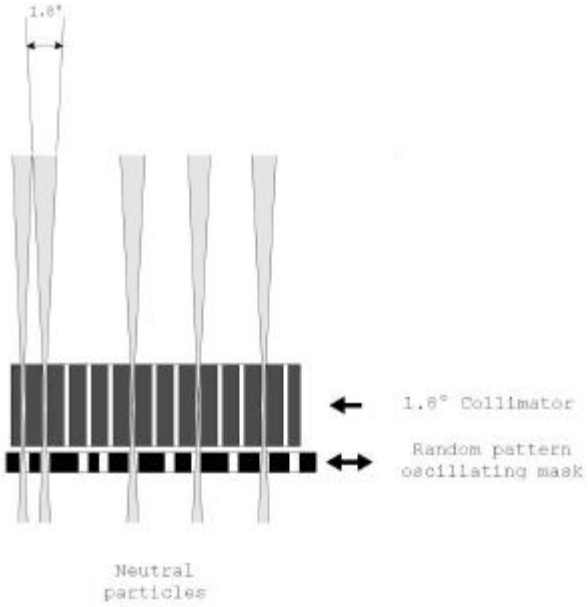

Figure 8. ELENA shuttering concept

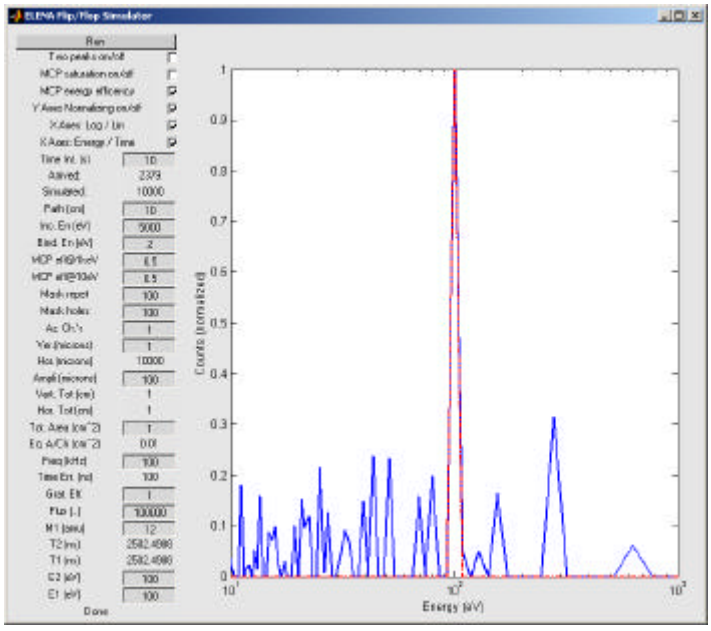

Figure 6. Sample Hadamard transform simulator for ELENA

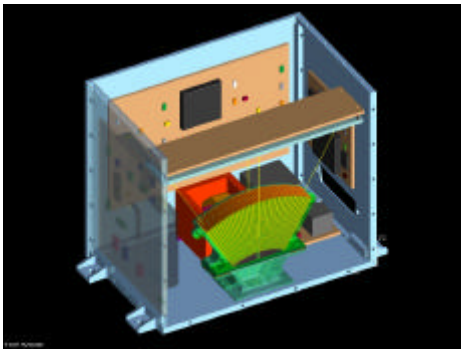

Figure 9. ELENA internal layout. Focusing optics and stop MCP on top.

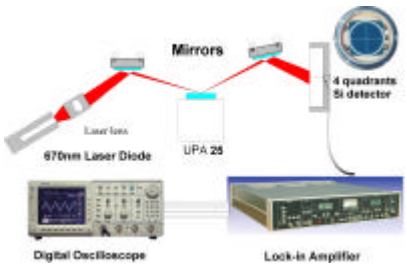

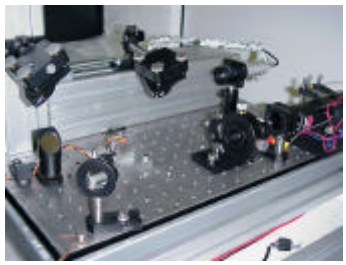

Figure 7. ENA-Piezo engine tested at CNR-ISM Microscope scanning facility (Courtesy of S. Selci) . The piezo is modulating a 670 nm laser beam onto a four quadrant tracker. The electrical converted modulated beam output is compared by a Lock-in amplifier (right picture) with the engine exciting frequency signal Short time tests show an equivalent stability of better than 1ns (250 sine waves) Long time tests – 1hour- better than 5 ns overall deviation.

1.3. MINI-DPU RATIONALE

The NPA package includes a common DPU electronics equipped with a DSP microprocessor and data storage blocks, which provides instrument operations control and loss-less data compression by a factor of about two. It will also be possible to switch to a lossy compression with a configurable error parameter. Due to the limited dimensions and budgets of the baseline DPU such remote sensor controller is envisaged to be hosted within system or common payload electronics units. The microprocessor performs about 200 MIPs, and requires about 600 mW. In the following we discuss in some detail the possible architectures for a miniaturized Digital processing units (DPUs) suitable as payload Data Handling Support Unit (DHSU) unit.

High computational power DPUs design techniques for space application mainly rely on two strategies: base the development around a well proven and qualified processor family or develop computational blocks in a hardware description language scaling its performances on the available target technology. Even if many example of compact DPU realized by applying the first methodology, the functional cores of the second category directly developed in hardware description language seem to be one of the promising ways for implementing powerful computational blocks independent of the specific H/W platform. Such approach has the advantage to scale the computational performances to the latest radiation-tolerant technology available from the ASIC and FPGA space market. For example the following developments:

- ESA - SPARC architecture LEON CPU http://www.estec.esa.nl/wsmwww/leon
- ESA - ERC32 SPARC V7 CPU http://www.estec.esa.nl/wsmwww/erc32
- Atmel - ERC32 SPARC part # TSC695E http://www.atmel-wm.com/products

have been already addressed for several applications and will be certainly used in many future projects. Other benefits of this practices concern the architectural reusability, the architectural extensibility and also the software components reusability.

By the way, the present qualified size of the H/W device (e.g. ACTEL has announced to release by next June 2003 a new rad-tolerant 300k gates FPGA) on which this kind of computational blocks can be synthesized is presently limited. This clearly indicates that such processors have and will have for the next future limited performances capabilities when memory and interfaces support have to be also accounted for. Moreover the relevant parameter which must be considered at payload level is the power consumption which - for such large scale integration devices - becomes a the major constraint. A more suitable approach is complementary to the above ones. It relies on the evidence that the Information Technology (IT) revolution has pushed tremendous investments and efforts for designing outstanding digital signal processor (DSP) devices as far as computational resources, power consumption, embedded memory resources, I/F flexibility are concerned, and for which the performances are far beyond any custom made assembling of similar chipset assembly of discrete parts. So far, the main strategy for a high performances payload DHSU is to largely benefit of such high grade of industrial developments, designing a μDPU assembly with specific cares, protections and qualification activities bringing up the radiation tolerance, the reliability and the operability of such devices to the requested level of this planetary space application. An example of such development is given in the following paragraph.

1.3.1 The 3^{Cube} MINI-DPU example

The main aim of this program (developed by AMDL Srl - Italy and financially supported by INAF/IFSI-Italy) was to offer to the Planetology Community an highly integrated self consistent processing unit capable to offer large computational resources, local memory reservoir, and to be able to support multi-sensors heads payload sustaining very high up/down transfer data rates for on-line or off line extended data processing support.

The 3^{Cube} *MINI-DPU* block is based on the state of the art of the DSPs developed in the frame of UMTS mobile technology research, which have been adapted in a high reliability design for space and harsh environment target applications. Such line of DSPs is offering superior performances and processing capability as high as 400 MIPS with power consumption lower than 50microW / MIPS. In the same block provision of 4M x 16 DRAM and 1M x 16 FLASH mass memory has been also given together with most popular solid state memories interfaces as *Media Card* and *Memory Stick*. A 10k gates general purpose FPGA has been also integrated, that can be externally configured and adapted to user specific applications. All components inside have been selected to be operated in the range -40 ÷

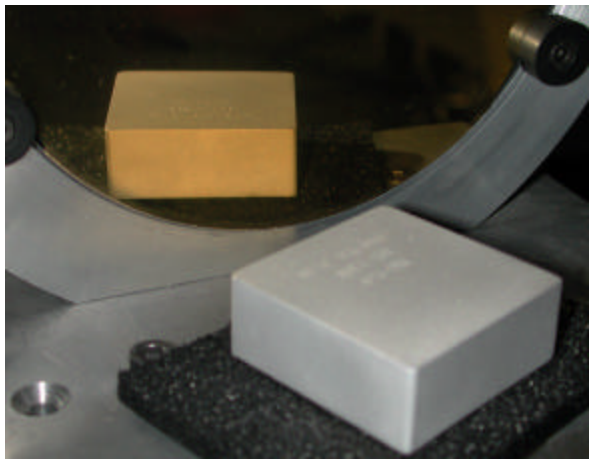

Figure 10. A view of 3^{Cube} *MINI-DPU* part.no MDSP_3CB_M003 proto-qualification model.

+85 °C and the intrinsic components radiation hardness performances can be extended by internal Indium/ Tantalum protection layers.
The *3Cube MINI-DPU* line has been already recognized to be the baseline solution as payload control unit in submitted proposals on ExoMars-Pasteur (3-Cube), Planetary Microprobes (DALOMIS).
The *3Cube MINI-DPU* has the following features:

- DSP operating up to 200 MHz (*Model 3MD-G*) or up to 120 MHz (*Model 3MD-P*)
- 4 Meg x 16 DRAM
- 1 Meg x 16 Flash Memory
- 32 Kilobyte SPI Flash Memory
- 10k gates customer programmable FPGA for user target I/F
- Universal Serial Bus (USB) interface
- Media Card MMC™ and Memory Stick MS™ interfaces available
- Embedded 1149.1 JTAG Emulation
- I^2 bus I/F
- 3 x 100Mbit/s bi-directional serial buses
- +5 volt operations
- 4 x 10 bit ADC channels (*Model 3MD-G*), 2 x 10 bit ADC (*Model 3MD-P*)
- PGA100, 0.1" pitch 100 pin interface

Moreover the *3Cube MINI-DPU* accounts for a very fast reservoir of about 196 kbytes of SARAM on which one access per cycle (one read or one write) can be performed.
The *3Cube MINI-DPU* has developed with a custom technology for growing the three dimensional stack of the parts.
Apart for the multi-layered passive shields the unit can accommodate internally the Single Event Latch-up (SEL) protection relays on the power handling of the internal power distribution which features thermal protection, multi point internal current limiters and power good processing for resetting and shutting down the system when any significant deviation from the powered domains is H/W detected. In the following pictures we give some evidence of the valuable low-power consumption of the system, which uses the state of the art of DSPs technology and associated electronics adapted in this particular case to the Mars environment.

Item	**Figure**
Weight (nude)	20 g
Power	500 mW(Max Power rate) / 100mW (stand-by)[1)]
Dimensions	3x3x0.5 cm^3 [2)]

[1)] Figure refers to a 240 MIPS case. The intrinsic core clock can be down clocked up to DC. As a rough figure 50µW/MIPS can be used in place for the computational core.
[2)]Customized development can be accounted for reducing further the size.

Table 1. Summary table for the *3Cube* like expected DHSU DPU budgets

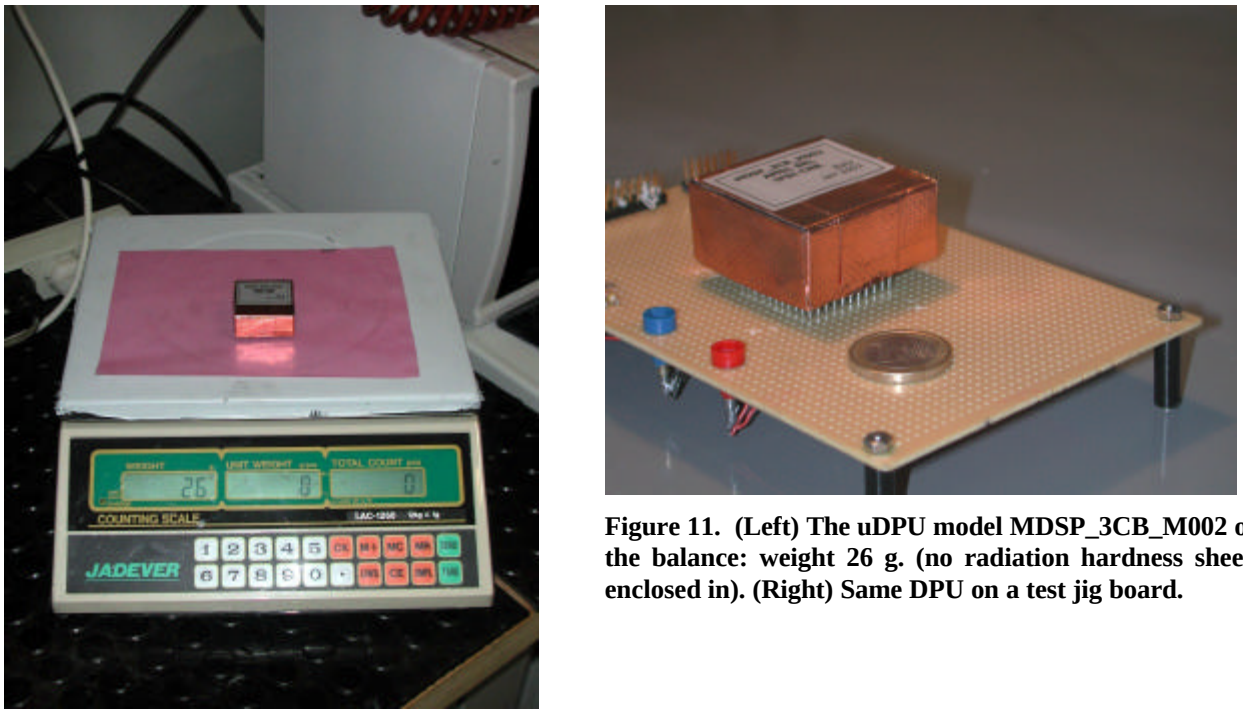

Figure 11. (Left) The uDPU model MDSP_3CB_M002 on the balance: weight 26 g. (no radiation hardness sheets enclosed in). (Right) Same DPU on a test jig board.

Figure 12. Right panel: uDPU in stand-by (100mW on primary). Left panel the uDPU during memory test (500 mW on primary).

References:

Cheng, A. F., E. P. Keath, S. M. Krimigis, B. H. Mauch, R. W. McEntire, D. G. Mitchel E. C. Roelof, D.J. Williams; Imaging neutral particle detector. Rem. Sens Rewiews, 8, 101–145, 1993.

Delcourt, D. C., T. E. Moore, S. Orsini, A. Millilo, and J.-A. Sauvaud, Centrifugal acceleration of ions near Mercury, GRL, June, 2002.

Funsten, H. O., D. J. McComas, B. L. Barraclough, E. E. Scime ; Ultra thin foils used for low-energy neutral atom imaging of the terrestrial magnetosphere, Opt. Eng. 32 (12), 3090–3095, 1993.

Funsten, H. O., D. J. McComas, E. E. Scime; Comparative study of low-energy neutral atom imaging techniques, Opt. Eng. 33 (2), 349–356, 1994.

Ip, Wing-Huen, A. Kopp, MHD simulations of the solar wind interaction with Mercury 10.1029/2001JA009171, 07 November 2002

Killen, R.M., Source and maintenance of the argon atmospheres of Mercury and the moon, Meteoritics and Planetary Science, 37, 1223 – 1231, 2002

Mildner, M., P. Wurz, S. Scherer, M. Zipperle, K. Altwegg, P. Bochsler, W. Benz, H. Balsiger, Measurement of neutrals atoms and ions in Mercury's exosphere, Planet. Space Sci., 49,, 2001.

Orsini, S., P. Cerulli-Irelli, M. Maggi, P. Baldetti, M. Candidi, G.Bellucci, A. Milillo, G. Chionchio, R. Orfei, S. Livi, I.A. Daglis, B. Wilken, W. Guttler, C. C. Curtis, K. C. Hsieh, J. Sabbagh, E. Flamini, E. C. Roelof, C. C. Chase, M. Grande, Imaging the Earth's magnetosphere: measuring energy, time-of-flight, and direction of Energetic Neutral Atoms with the ISENA instrument, *AGU Monograph 103: Measurements Techniques in Space Plasmas: Fields*, ed. by R. F. Pfaff, J. E. Borovsky, and D. T. Young, 269–274, 1998.

Orsini, S., A. Milillo, E. De Angelis, A. M. Di Lellis, V. Zanza, S. Livi; Remote sensing of Mercury's magnetospheric plasma environment via energetic neutral atoms imaging; Plan. Space Sci, 49, 1659–1678, 2001.

Potter, A.E., R.M. Killen and T.H. Morgan, The sodium tail of Mercury Meteoritics and Planetary Science, 37, 1165–1172, 2002

Potter, A.E., C.M. Anderson, R.M. Killen and T.H. Morgan, Ratio of sodium to potassium in the Mercury exosphere, Journal of Geophysical Research (planets), Nov., 2002

Rème H., J. M. Bosqued., J. A. Sauvaud, A. Cros, I. Dandouras, C. Aoustin, J. Boyssou, Th. Camus, J. Cuvilo, C. Martz, J. Mèdale, H. Perrier, D. Romefort, J. Rouzaud, C. d'Uston, E. Moubius, K. Crocker, M. Granoff, L. M. Kistler,, M. Popecki, D. Hovestadt, B. Klecker, G. Paschmann, M. Scholer, C. W. Carlson, D. W. Curtis, R. P. Lin, J. P. McFadden, V. Formisano, E. Amata, M. B. Bavassano-Cattaneo., P. Baldetti, G. Bellucci, R. Bruno, G. Chionchio, A. M. Di Lellis, E. G. Shelley, A. G. Ghielmetti, W. Lennartsson, A. Korth, H. Rosenbauer, R. Lundin, S. Olsen, G. K. Parks, M. McCarthy, H. Balsiger, The Cluster ion spectrometry (CIS) experiment; Space Sciences Review Vol. 79, Nos 1–2 1997.

Slater, D. C., ASPERA ELS UV Suppression Study Final Report, Southwest Research Institute, 2000

Wurz, P.; Detection of energetic neutral particles, the outer heliosphere: beyond the planets, (eds. K. Scherer, H. Fichtner, and E. Marsch), Copernicus Gesellschaft e.V., Katlenburg-Lindau, Germany, 251–288, 2000.

Submitted papers

Delcourt, D. C., S. Grimald, F. Leblanc, J.-J. Berthelier, A. Millilo, A. Mura, and S. Orsini, A quantitative model of planetary Na+ contribution to Mercury's magnetosphere, submitted to Annales Geophys.

Kallio, E., and P. Janhunen, Modelling the Solar Wind Interaction with Mercury by a Quasineutral Hybrid Model, submitted to Annales Geophysicae.

Killen, R.M., M. Sarantos and P. Reiff., Space Weather at Mercury, submitted to Advances in Space Research**.**

Lammer, H, P. Wurz, M. R. Patel, R. Killen, C. Kolb, S. Massetti, S. Orsini, and A. Milillo, The variability of Mercury's exosphere by particle and radiation induced surface release processes submitted to Icarus.